



Biomimetic organohydrogel actuator with high response speed and synergistic fluorescent variation

Hui Shang^{a,b}, Xiaoxia Le^{a,c}, Muqing Si^{a,c}, Shuangshuang Wu^{a,c}, Yu Peng^{a,c}, Fuqing Shan^a, Si Wu^d, Tao Chen^{a,c}

^a Key Laboratory of Marine Materials and Related Technologies, Zhejiang Key Laboratory of Marine Materials and Protective Technologies, Ningbo Institute of Material Technology and Engineering, Chinese Academy of Sciences, Ningbo 315201, China

^b Nano Science and Technology Institute, University of Science and Technology of China, No. 166 Renai Road, Suzhou 215000, China

^c School of Chemical Science, University of Chinese Academy of Sciences, 19A Yuquan Road, Beijing 100049, China

^d Department of Polymer Science and Engineering, University of Science and Technology of China, No. 96 Jinzhai Road, Hefei 230026, China

ARTICLE INFO

Keywords:

Organohydrogel actuator
Stimuli responsive
Fluorescence variation
Fast morphing

ABSTRACT

Current hydrogel-based actuators have achieved rapid development due to their excellent performance such as shape-morphing and color-changing for application in fields such as camouflage, biomimetic soft-robotics and so on. However, it is still challenging to fabricate soft robots with the capability of simultaneous changes in shape and fluorescent color at a fast speed when triggered by one single stimulus. Herein, an anisotropic organohydrogel actuator made up of rGO-doped hydrophilic poly(N-isopropylacrylamide) (PNIPAM) network and hydrophobic poly(lauryl methacrylate) (PLMA) network is prepared via a two-step interpenetrating method. Bearing fluorescent monomer N-(4-(1,2,2-triphenylvinyl)phenyl)acrylamide (ATPE) as well as fluorescent ligand 6-acrylamidopicolinic acid (6APA), the PLMA network shows fluorescent changes in color or brightness depending on the presence or absence of Eu^{3+} ions in response to heat/NIR. In a word, the proposed organohydrogel actuator, which exhibits simultaneous fluorescence color variation and fast morphing in response to one stimulus, provides insights in designing and fabricating novel soft robots.

1. Introduction

Stimuli-responsive hydrogels, possessing the capacity of morphology alteration or color variation when exposed to external stimuli, have shown various applications in fields of soft actuators [1–4], biological medicine [5,6], information storage [7,8], sensors [9,10], etc. Among them, hydrogel actuators with synergetic color changes have aroused great attention due to their unique ability to imitate living organisms (chameleons, flowers, cephalopods, etc.) for surviving in their environment. From the methods of constructing anisotropic structures [11–14], including bilayer structure, oriented structure, and gradient structure, to the introduction of different luminescent forms, much effort has been devoted to endow soft-robotics with color change performance [15–19]. Previously, our group has developed a bilayer hydrogel actuator consisting of a thermo-responsive GO-PNIPAM layer and pH-responsive PBI-HPEI layer, leading to the abovementioned synergistic functions [20]. More recently, a hydrogel actuator with both color-changing and shape-morphing capabilities has been developed, which was based on supramolecular dynamic metal–ligand coordination under

the subtle interplay between acidity/alkalinity, metal ions, and temperature [21].

Though above attempts achieved the coexistence of shape alteration and fluorescence variation in one system, the change in either fluorescence color or shape is triggered by different stimuli. Therefore, it is still challenging to construct a hydrogel actuator with simultaneous fluorescence variation based on one single stimulus. In order to realize this goal, Tang et al. had developed hydrogels with simultaneous changes in fluorescence, brightness and shape in response to a single stimulus of pH by using aggregation-induced emission luminogen, tetra-(4-pyridylphenyl)ethylene (TPE-4Py), as a core function fluorescence element [22]. Zhou's group has also reported a novel lanthanide-ion-coordinated supramolecular hydrogel, which can respond to different humidity or hydration/dehydration conditions within dynamical variation of luminescence and opacity [23]. However, these systems are still lacking in response speed due to the difficulties in altering pH or humidity.

The development of heterogeneous organohydrogel [24], which was made up of both hydrophilic and hydrophobic monomers and can swell in either water or oil, provides a new inspiration for obtaining hydrogel

E-mail addresses: lexiaoxia@nimte.ac.cn (X. Le), tao.chen@nimte.ac.cn (T. Chen).

<https://doi.org/10.1016/j.cej.2021.132290>

Received 19 July 2021; Received in revised form 28 August 2021; Accepted 3 September 2021

Available online 6 September 2021

1385-8947/© 2021 Elsevier B.V. All rights reserved.

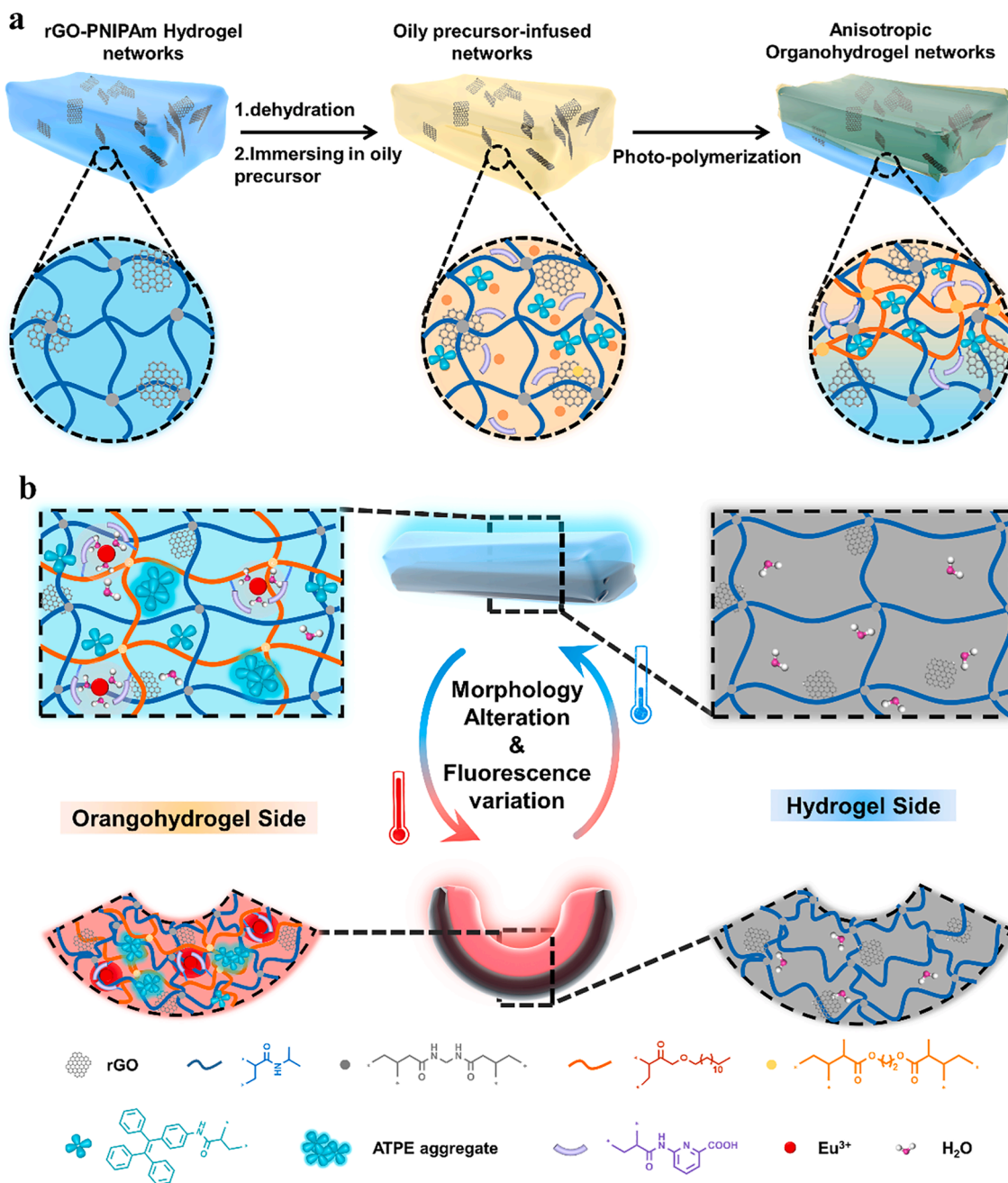


Fig. 1. (a) The preparation process of a fluorescent rGO-PNIPAM/P(LMA-ATPE-6APA) organohydrogel actuator using a hydrogel network as the scaffold to incorporate organogel network via a two-step interpenetrating method. (b) Schematic illustration of anisotropic rGO-PNIPAM/P(LMA-ATPE-6APA) organohydrogel actuator doped with Eu³⁺ ions, showing simultaneous fluorescence color change as well as complex shape deformation in response to external stimuli such as heat or NIR.

actuators with simultaneous fluorescence change for the following two reasons. Firstly, the two-step interpenetrating technique, which includes a free radical polymerization process and photo-polymerization procedure, lays the foundation for realizing anisotropic structures by controlling the irradiation time. Furthermore, the coexistence of a hydrophobic network and hydrophilic network provides a convenience way for the introduction of oily fluorescent monomers without having to consider aggregating problems. Herein, we developed an organohydrogel exhibiting simultaneous fluorescence change (intensity or color) and fast actuation under one single stimulus of heat/NIR. Specifically, thermal-responsive PNIPAM hydrogel containing rGO sheets was firstly prepared via radical polymerization within the UV-induced reduction process of GO. Through a two-step interpenetrating process,

the hydrophobic organogel network was introduced *via* time-controlled photo-polymerization, leading to a fluorescent organohydrogel actuator with anisotropic structure (Fig. 1a). As shown in Fig. 1b, due to the differences in deswelling rates of the organohydrogel's two sides, the initially straight strip could be bend into a circle shape when exposed to heat or NIR. In the meanwhile, ATPE fluorophores on the hydrophobic network, which exhibit aggregation induced emission (AIE) behavior, dramatically enhanced its intensity when PNIPAM polymer chains shrink above the lower critical solution temperature (LCST). In addition, once Eu³⁺ ions are introduced and coordinate with the fluorescent ligand 6APA to form the 6APA-Eu³⁺ complex, the organohydrogel can be endowed with red fluorescence emission, leading to fluorescence transition from blue to red after the application of thermal stimulation.

Furthermore, as rGO possess the ability to display the photothermal effect, the organohydrogel actuator which exhibits fluorescence emissions varying from blue to red can be remotely controlled. As a result, a hydrogel actuator with both high response speed and fluorescence variation such as brightness or emission color can be achieved, acting as an attractive material in the field of biomimetic soft-robotics.

2. Experimental section

2.1. Materials

N-isopropylacrylamide (NIPAM, $\geq 98\%$) were purchased from TCI (shanghai) reagent Co. Ltd. Ethylene glycol dimethacrylate (EGDMA, $\geq 98\%$), 2,2-diethoxyacetophenone (DEAP, $\geq 95\%$), ammonium persulfate (APS, $\geq 98\%$), *N,N'*-Methylene bis(acrylamide) (BIS, $\geq 98\%$), *N,N,N',N'*-Tetramethylethylenediamine (TEMED) were commercially provided by Aladdin reagent Co. Ltd. Acryloyl chloride ($\geq 99.0\%$) was gotten from J&K Scientific Ltd. Triethylamine ($\geq 99.0\%$), ethyl acetate ($\geq 99.5\%$), sodium hydroxide (NaOH, 96.0%), and hydrochloric acid (HCl) were obtained from Sinopharm Chemical Reagent Co. Ltd. Triethylamine, dry dichloromethane and $\text{Eu}(\text{NO}_3)_3 \cdot 6\text{H}_2\text{O}$ (99.9%) were commercially supplied by Energy Chemical Co. Ltd. 4-(1,2,2-triphenylvinyl)aniline (TPE, 97%) was purchased from Zhengzhou JACS Chem Product Co. Ltd. Lauryl methacrylate (LMA) was purchased from Shanghai Macklin Biochemical Co. Ltd. All reagents were used without any treatment or purification.

2.2. Synthesis of fluorescent monomer *N*-(4-(1,2,2-triphenylvinyl)phenyl)acrylamide (ATPE):

ATPE was synthesized in accordance with our previous report and the synthetic route was shown in Fig. S1. TPE (2 g) was firstly dissolved in a mixed solution of dry dichloromethane (10 mL) and triethylamine

(5 mL). Then, acryloyl chloride (1 mL) was mixed with dry dichloromethane (4 mL) before adding dropwise into above solution under N_2 protection at 0°C . After stirring for another 3 h at room temperature, the product was obtained by being successively extracted with hydrochloric acid (0.02 M), saturated sodium hydrogen carbonate solution and dried by rotary evaporat.

2.3. Preparation of rGO-PNIPAM hydrogel:

2 g NIPAM, 2.4 mg BIS (0.12 wt% of NIPAM), 20 mg APS (1 wt% of NIPAM) were firstly dissolved in 10 mL water containing GO (0.5 mg/mL). Then, 20 μL TEMED was added into above solution, and the mixed solution was oscillated rapidly before being transferred into home-made molds. After polymerization for 8 h, the GO-PNIPAM hydrogel was exposed to UV light (50 W) for reducing to rGO-PNIPAM hydrogel. At last, the obtained hydrogel was put into acetone to for removing unreacted monomers.

2.4. Preparation of rGO-PNIPAM/P(LMA-ATPE-6APA) organohydrogels:

Organogel precursor solution containing 20 mL LMA, 10 mL ethanol, 150 μL EGDMA, 0.1 g DEAP, 0.06 g ATPE and certain amount of 6APA were firstly prepared. Dehydrated gels were immersed into precursor solution for 10 h before being sandwiched between two pieces of quartz glasses without air bubbles. After being irradiated by UV light (365 nm, 50 W) for a certain time, the prepared organohydrogels were put into ethanol for getting rid of unreacted monomer and finally being swelled in deionized water for solvent replacement.

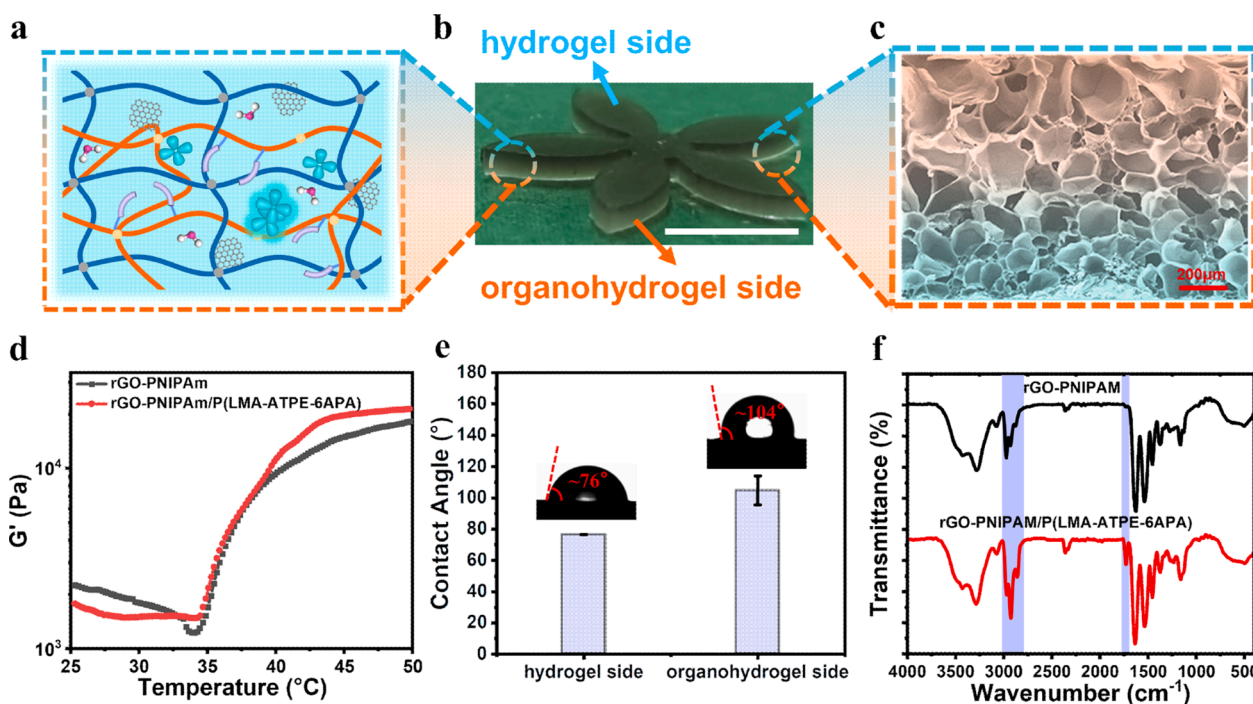


Fig. 2. The characterization of anisotropic rGO-PNIPAM/P(LMA-ATPE-6APA) organohydrogel. (a) Cross-sectional schematic of anisotropic rGO-PNIPAM/P(LMA-ATPE-6APA) organohydrogel actuator. (b) The photograph of organohydrogel. Scale bar: 1 cm. (c) Cross-sectional SEM image of rGO-PNIPAM/P(LMA-ATPE-6APA) organohydrogel. (d) The storage modulus (G') on a temperature sweep ($2^\circ\text{C}/\text{min}$) at a constant shear strain of 1% and frequency of $10\text{ rad}\cdot\text{s}^{-1}$ of rGO-PNIPAM hydrogel and anisotropic rGO-PNIPAM/P(LMA-ATPE-6APA) organohydrogel. (e) Contact angles for both the organohydrogel side and hydrogel side of the anisotropic rGO-PNIPAM/P(LMA-ATPE-6APA) organohydrogel actuator. (f) ATR spectra of pure rGO-PNIPAM hydrogel and anisotropic rGO-PNIPAM/P(LMA-ATPE-6APA) organohydrogel.

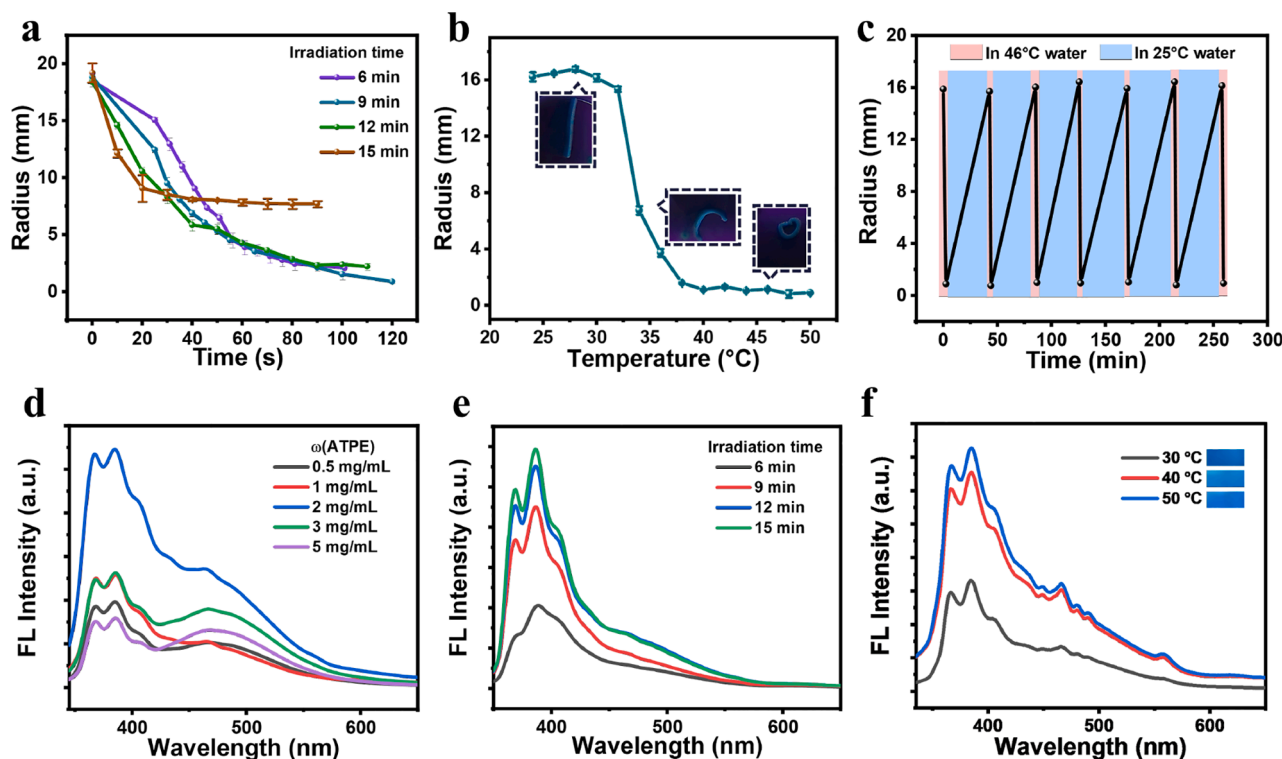


Fig. 3. The actuating and fluorescent performance of the rGO-PNIPAM/P(LMA-ATPE-6APA) organohydrogel actuators. (a) The actuating degree of various anisotropic rGO-PNIPAM/P(LMA-ATPE-6APA) organohydrogels prepared by exposing them to a UV lamp with different time (6, 9, 12 and 15 min) in 46 °C water. (b) The actuating degree of organohydrogel prepared by 9 min of UV irradiation with temperature variation. (c) Anisotropic rGO-PNIPAM/P(LMA-ATPE-6APA) organohydrogel prepared by 9 min of UV irradiation cyclically actuating in water at 20 °C and 46 °C, respectively. (d) The fluorescence spectra of anisotropic rGO-PNIPAM/P(LMA-ATPE-6APA) organohydrogels with different amounts of ATPE, which were prepared by soaking in various oily precursor solutions containing different concentrations of ATPE (0.5, 1, 2, 3 and 5 mg/mL). (e) The fluorescence spectra of different anisotropic rGO-PNIPAM/P(LMA-ATPE-6APA) organohydrogels, which were prepared by immersion in the same oily precursor solution (2 mg/mL ATPE) but exposed to UV light with varying time (6, 9, 12 and 15 min). (f) The fluorescence intensity of anisotropic rGO-PNIPAM/P(LMA-ATPE-6APA) organohydrogel (2 mg/mL ATPE, 9 min) at different temperature of 30 °C, 40 °C and 50 °C.

2.5. Preparation of rGO-PNIPAM/P(LMA-ATPE-6APA-Eu³⁺) organohydrogel:

For the preparation of rGO-PNIPAM/P(LMA-ATPE-6APA-Eu³⁺) organohydrogels, rGO-PNIPAM/P(LMA-ATPE-6APA) organohydrogels were immersed in a solution of Eu³⁺ solution (0.1 M) for 15 min, and then placed in deionized water to remove excessive Eu³⁺ for another 5 h.

2.6. Characterization

¹H NMR spectra were obtained from a Bruker Avance III 400 MHz spectrometer. UV-Vis absorption and transmittance spectra were measured on an UV-Vis spectrophotometer (TU-1810, Purkinje General Instrument Co. Ltd.). ATR-FTIR spectra was recorded on a Thermo Scientific Nicolet 6700 FT-IR spectrometer. The digital photos of the polymeric films were taken under a UV lamp (ZF-5, 5 W, 254 nm). All fluorescent photographs were taken using the same UV lamp. Steady-state fluorescence measurements were obtained from a Hitachi F-4600 fluorescence spectrofluorometer at room temperature and a HPRIBA FL3-111 fluorescence spectrofluorometer at higher temperature with a 500 W Xenon lamp. The excitation wavelength was 254 nm and the scan speed was 1200 nm/min. The cross-section morphology of the polymeric hydrogel and organohydrogel were performed by a field-emission scanning electron microscopy (SEM, S-4800, Hitachi) with an accelerating voltage of 8.0 kV. The chemical bonding and bonding state were measured by Raman using a Renishaw inVia Reflex instrument. Microscopic images were obtained from an OLYMPUS BX51 polarizing microscope. All water contact angle was measured using Dataphysics OCA25 instrument by carefully dropping a 3 μ L water droplet on the

surface of a fabricated organohydrogel. At least three different spots of the same sample surface were recorded to receive the mean value.

3. Results and discussion

3.1. Fabrication of rGO-PNIPAM/P(LMA-ATPE-6APA) organohydrogel

The fluorescent monomer ATPE and fluorescent ligand 6APA were firstly prepared according to previous work [21]. At the same time, the fluorescent monomer ATPE showing typical AIE performance was synthesized and characterized (Figs. S1-S3). In order to prove that there is no photobleaching phenomenon of fluorescent monomers in the process of UV illumination for a short time such as 9 min, UV absorption spectra of ATPE solution were recorded (Fig. S4). The hydrogel network was constructed through polymerization of NIPAM in the presence of graphene oxide (GO), N,N'-Methylene bis(acrylamide) (BIS, crosslinker) and ammonium persulfate (APS, initiator). In order to obtain a better photothermal effect, the prepared GO-PNIPAM hydrogel was reduced to a rGO-PNIPAM hydrogel by the irradiation with a UV lamp (50 W) for 8 h (Fig. S5 and Fig. S6) [20]. After being dehydrated in acetone, the rGO-PNIPAM gel was immersed in an oily precursor solution containing the main monomer lauryl methacrylate (LMA), the fluorescent monomer ATPE and the fluorescent ligand 6APA. As the penetration of UV light is limited by distance, by controlling the time of photo-polymerization, an elaborate organohydrogel-based actuator, exhibiting simultaneous fluorescence brightness/color change and fast shape deformation under one single stimulus of heat/NIR, was obtained (Fig. S7).

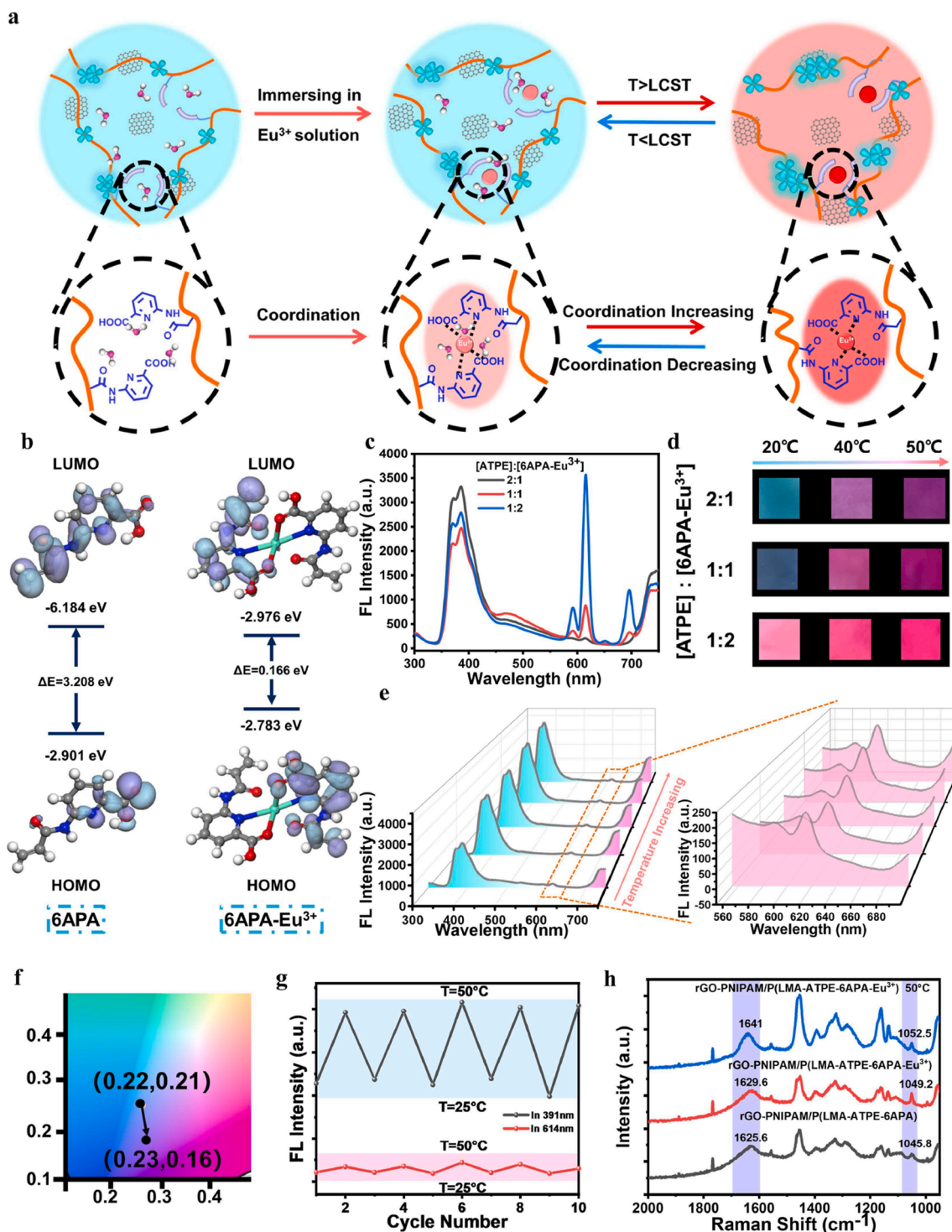


Fig. 4. The fluorescence changes of the rGO-PNIPAM/(LMA-ATPE-6APA-Eu³⁺) organohydrogel. (a) Schematic of fluorescence color change of Eu³⁺-doped organohydrogel before and after heating. (b) The energies of HOMO and LUMO of 6APA before and after coordinating with Eu³⁺. (c) The fluorescence spectra and (d) photographs of the anisotropic rGO-PNIPAM/(LMA-ATPE-6APA-Eu³⁺) organohydrogels containing different content of 6APA for tuning the ratios of two fluorescent monomer/ligand. (e) The fluorescence spectra of organohydrogel with temperature increasing when the ratios of two fluorescent monomer/ligand fixed at 2:1. (f) The fluorescence color change of organohydrogel before and after heating at a CIE diagram. (g) The circular changes of fluorescence intensity at 391 nm (black) and 614 nm (red) by adjusting temperature at 25 °C and 50 °C. (h) Raman spectra of anisotropic rGO-PNIPAM/(LMA-ATPE-6APA) organohydrogel and anisotropic rGO-PNIPAM/(LMA-ATPE-6APA-Eu³⁺) organohydrogel before and after employing thermal stimulation. (For interpretation of the references to color in this figure legend, the reader is referred to the web version of this article.)

3.2. Anisotropic structural characterization of prepared organohydrogel

The prepared rGO-PNIPAM/P(LMA-ATPE-6APA) organohydrogel shows an obvious anisotropic structure, which can be directly confirmed

both macroscopically and microscopically (Fig. 2a-2c). As LMA was introduced into the rGO-PNIPAM hydrogel network, hydrophobic microdomains would form when the solvent was completely replaced by water, and the gel shows a color gradient from black (on the hydrogel

side) to gray to white (on the organohydrogel side). In the meanwhile, compared with pure rGO-PNIPAM hydrogel (Fig. S8), the porous structure of the organohydrogel with varying sizes was investigated by Scanning Electron Microscope (SEM), proving the successful introduction of organogel network. Furthermore, the anisotropic structure could also be easily observed due to the difference in contrast via optical microscope (Fig. S9). At a slightly higher transformation temperature, the organohydrogel also exhibited a more rapid and higher increase of storage modulus (G') according to a temperature sweep (Fig. 2d). There was a marked difference in the contact angle (CA) of two sides of rGO-PNIPAM/P(LMA-ATPE-6APA) organohydrogel (Fig. 2e). In comparison to the hydrogel side with a CA of 76° , the organohydrogel side displayed a bigger CA of 104° , which also indicates the anisotropic structure of the prepared organohydrogel. To verify the chemical composition and structure of the hydrogel and organohydrogel, both rGO-PNIPAM hydrogel and rGO-PNIPAM/P(LMA-ATPE-6APA) organohydrogel were measured by attenuated total reflection Fourier transformed infrared spectrometer (ATR-FTIR). As shown in Fig. 2f, within similar spectra, some new peaks appeared in that of rGO-PNIPAM/P(LMA-ATPE-6APA) organohydrogel (red line). The emerging absorption peak at 1728 cm^{-1} was attributed to the presence of C=O groups in PLMA polymer chains, and the significantly enhanced peaks at 2923.5 cm^{-1} were caused by the asymmetric stretching of $-\text{CH}_2-$ groups. These can be assigned to the hydrophobic PLMA polymer chains, which illustrates the successful introduction of PLMA into the rGO-PNIPAM hydrogel matrix.

3.3. Simultaneous fast morphing and fluorescent brightness variation of organohydrogel

Our anisotropic structure was obtained by controlling the time of UV irradiation during the photo-polymerization process[25]. As shown in Fig. 3a, the actuating speed and driving degree of the organohydrogel actuators vary with the time of photo-polymerization. Among them, the anisotropic organohydrogel actuators fabricated by a UV light exposure of 9 min possessed both fast driving ability and large actuation variation, showing curvature alteration from 20 mm to 2.5 mm in 80 s. Therefore, organohydrogel prepared by 9 min of UV irradiation was selected as the target actuator. As it can be seen in Fig. 3b, the organohydrogel sheet can adjust its bending angle in response to warm water due to the anisotropic structure, showing a transition temperature range from 31°C to 38°C . The thermal-induced shape deformation performance is completely reversible and can be repeated at least 6 times without any obvious changes (Fig. 3c), which indicates the good stability of our organohydrogel.

As one of the typical AIEgens, the fluorescent monomer ATPE shows significant changes in fluorescence intensity before and after aggregation[26–28], which can be easily achieved in our system by thermal-induced phase transition of PNIPAM chains. Continuous hydrophobic phase in the heterogeneous structure of our organohydrogel lays a foundation for the introduction of hydrophobic fluorescent monomer (ATPE) as well as fluorescent ligand (6APA), that was going to be used in the following studies. Through adjusting the concentration of ATPE (2 mg/mL) in the oily precursor solution as well as the irradiation time for polymerization process (9 min), the fluorescence intensity can be regulated to optimum while taking the actuation performance into consideration (Fig. 3d and Fig. 3e). Determined by the characteristic peak of ATPE in the UV-Vis absorption spectra (Fig. S11), the organohydrogel can emit blue fluorescence in response to a certain wavelength (254 nm), which can be further tuned by temperature changes. As illustrated in Fig. 3f, the fluorescence intensity can be dramatically enhanced when the temperature is increased from 30°C to 50°C , and is accompanied by a color change from cyan to blue by visual inspection (Fig. S12). These all can be derived from the shrinkage of the PNIPAM polymeric network, resulting in an increase of aggregation degree of ATPE in the organogel network. As a proof-of-concept, the anisotropic organohydrogel was tailored into a flower shape, showing simultaneous

fast morphing and fluorescent brightness variation in warm water (46°C) (Fig. S13).

3.4. Fluorescent color change of Eu^{3+} -doped organohydrogel

Since the copolymerized monomer 6APA can coordinate with lanthanide ion such as Eu^{3+} and lead to red fluorescence emission under 254 nm (Fig. S14)[21], the organohydrogel doped with Eu^{3+} performed a fluorescence color variation during the process of temperature change. Owing to the attenuate hydration of Eu^{3+} and the enhanced coordination between 6APA and Eu^{3+} , the related organohydrogel showed a fluorescence color change from cyan to red with the increase of temperature (Fig. 4a). Molecular orbital amplitude plots of highest occupied molecular orbital (HOMO) and lowest unoccupied molecular orbital (LUMO) energy levels of 6APA, 6APA- Eu^{3+} complex and ATPE based on density functional theory (DFT) calculation are shown in Fig. 4b and Fig. S15 [29–31]. The separation degree of the electron cloud between HOMO and LUMO of 6APA is obviously larger than that of 6APA- Eu^{3+} , and the energy gap (ΔE) between HOMO and LUMO of 6APA- Eu^{3+} was less than that of 6APA, indicating that 6APA- Eu^{3+} is more susceptible towards excitation. Once Eu^{3+} was introduced into the system, the cyan fluorescent color of the original rGO-PNIPAM/P(LMA-ATPE-6APA) organohydrogel can be enriched by adjusting the molar ratio of ATPE and 6APA. As shown in Fig. 4c, the fluorescent color of the organohydrogel is altered from cyan to red when increasing the amount of 6APA, along with a decrease in FL intensity at 391 nm and an increase in FL intensity at 614 nm.

One interesting phenomenon of our system is the thermal-induced fluorescence color change, which happens when the ratio of ATPE and 6APA is appropriate. As shown in Fig. 4d, the fluorescent organohydrogel array displays a rich color variation through the control of temperature and proportion. When the molar ratio of ATPE to 6APA was fixed at 2:1, the organohydrogel shows the most striking color change with the temperature rising, from cyan to purplish-red, and was thus selected for further study. In addition, the color change can also be monitored by fluorescence spectra at varying temperatures (Fig. 4e, Fig. S16 and Fig. S17), showing a significant enhancement in both cyan fluorescence (350–450 nm) and red fluorescence (550–700 nm) during the heating procedure. It is worth mentioning that the fluorescent intensity ratios at 391 nm and 614 nm ($I_{391\text{ nm}}/I_{614\text{ nm}}$) decreased when the temperature was raised, leading to the cyan-red transition (Fig. S18). The Commission Internationale de L' Eclairage (CIE) coordinates of the selected organohydrogel before and after heating are (0.22, 0.21) and (0.23, 0.16), corresponding to cyan and purplish-red (Fig. 4f). What's more, owing to the good stability of our organohydrogel, the fluorescence color variation can be repeated at least 5 times in the process of temperature switching via recording the fluorescence intensity at 391 nm and 614 nm (Fig. 4g). The Raman spectrum of the rGO-PNIPAM/P(LMA-ATPE-6APA) organohydrogel and the rGO-PNIPAM/P(LMA-ATPE-6APA- Eu^{3+}) organohydrogel before and after employing thermal stimulation were demonstrated in Fig. 4h, through which the water-polymer interactions can be evaluated[21]. All the spectra were collected in the wavenumber range of $950\text{--}2000\text{ cm}^{-1}$ and analyzed separately in two spectral regions corresponding to C=O stretching ($1600\text{--}1700\text{ cm}^{-1}$) and vibrations of the pyridine rings ($1000\text{--}1100\text{ cm}^{-1}$) belonging to 6APA. The two peaks respectively located at 1045.8 and 1625.6 cm^{-1} both shifted to higher wavenumbers after integrating Eu^{3+} , indicating changes in the interactions between 6APA and water surrounding them due to the formation of 6APA- Eu^{3+} complex. Furthermore, the heating process can cause the shrinking of organohydrogel, leading to the enhancement of coordination strength between 6APA and Eu^{3+} that is manifested in the shifting of peaks towards even higher wavenumbers.

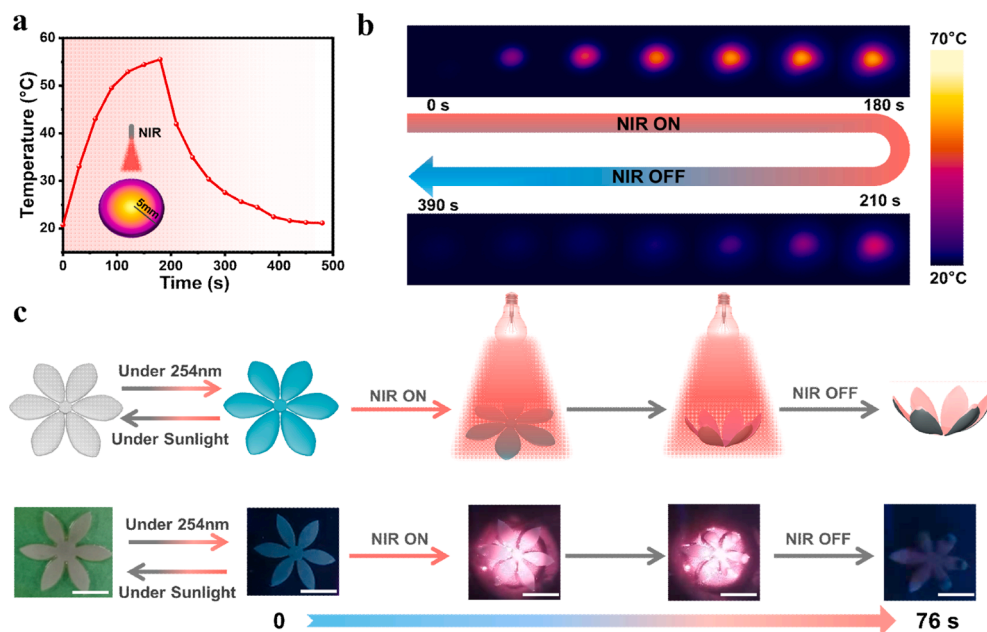


Fig. 5. Remotely controlled synergistic color-changing and shape-morphing of organohydrogel actuators. (a) The rising and cooling curves of the anisotropic rGO-PNIPAM/P(LMA-ATPE-6APA-Eu³⁺) organohydrogel obtained by turning on/off NIR light (808 nm, 0.478 W/cm²). (b) Pictures of temperature rising of anisotropic rGO-PNIPAM/P(LMA-ATPE-6APA-Eu³⁺) organohydrogel by using NIR laser. (c) Schematic diagram and photos of flower-shaped anisotropic rGO-PNIPAM/P(LMA-ATPE-6APA-Eu³⁺) organohydrogel showing synergistic fluorescence color alteration and fast shape deformation. Scale bar: 1 cm.

3.5. Remotely controlled synergistic color-changing and shape-morphing of organohydrogel

Due to great photothermal conversion efficiency of rGO, the resultant rGO-PNIPAM/P(LMA-ATPE-6APA-Eu³⁺) organohydrogel was imparted with remotely controlled synergistic color-changing and shape-morphing properties in response to NIR light. With the irradiation of NIR (808 nm, 0.478 W/cm²) for 180 s, the planar sheet of organohydrogel was heated to about 55 °C and can also recover to the initial shape within 300 s after removing the NIR light, which make it possible for organohydrogel actuators to conduct NIR-induced actuating performance (Fig. 5a). The process of heating and cooling can also be recorded more intuitively by IR images (Fig. 5b). As a proof-of-concept, a flower-shaped organohydrogel was studied as a model (Fig. 5c). When irradiated by NIR (808 nm, 0.678 W/cm²), the temperature of the flower-shaped organohydrogel could gradually increase, leading to the closure of the “flower” in 76 s. At the same time, the fluorescent color of the organohydrogel changed from cyan to purplish-red, which can be clearly observed after turning off the NIR light. With time going by, both the fluorescent color and shape of the organohydrogel can recover to its original state. This phenomenon can be attributed to the good photothermal effect of rGO as well as the inhomogeneous distribution of PLMA polymer chains that constructing an anisotropic structure. Once the temperature increased, PNIPAM polymer chains would shrink and discharge water, which led to the constriction of PLMA, thus resulting in the aggregation of ATPE and the enhancement of coordination between Eu³⁺ and 6APA. The ability of simultaneous fluorescence color change and fast shape deformation endows the organohydrogel actuator with a broader application space in the field of intelligent biomimetics.

4. Conclusions

In summary, an anisotropic organohydrogel actuator with abilities of simultaneous fluorescence color or brightness changes as well as fast shape deformation under one stimulus was fabricated through a two-step interpenetrating method. By controlling photo-polymerization time, the intelligent actuator can present fluorescence intensity enhancement due to the aggregation of ATPE moieties, which were caused by PNIPAM chains' contraction above the LCST. Once Eu³⁺ ions were introduced and coordinated with 6APA ligands, red fluorescence can be emitted due to the formation of the 6APA-Eu³⁺ complex.

Moreover, thermal-induced hydrophobicity of PNIPAM chains could contribute to the reduction of hydration between Eu³⁺ and H₂O, leading to an increase in red emission. As a result, an organohydrogel-based soft actuator with fast driving capability, along with fluorescence color variation from blue to red can be obtained. Our strategy of constructing anisotropic organohydrogel owning synergistic discoloration and actuation performance can inspire new ideas for fabricating hydrogel actuators, providing more possibilities for introducing various hydrophobic fluorescent monomers into hydrogel systems, and broadening the potential application fields of multifunctional soft robots.

Declaration of Competing Interest

The authors declare that they have no known competing financial interests or personal relationships that could have appeared to influence the work reported in this paper.

Acknowledgements

H. S. and X. L. contributed equally to this work. The authors thank Tim P. Mach from Karlsruhe Institute of Technology (KIT), Germany for his kind help with the revision to this manuscript. This work was supported by the National Natural Science Foundation of China (52103246, 51873223, 51773215, 21774138), National Key Research and Development Program of China (2018YFC0114900, 2018YFB1105100), China Postdoctoral Science Foundation (Grant Nos. 2020M671828), the Natural Science Foundation of Ningbo (202003N4361), Youth Innovation Promotion Association of Chinese Academy of Sciences (2017337), Key Research Program of Frontier Science, Chinese Academy of Sciences (QYZDB-SSW-SLH036), the Sino-German Mobility Program(M-0424), and K.C.Wong Education Foundation (GJTD-2019-13).

Appendix A. Supplementary data

Supplementary data to this article can be found online at <https://doi.org/10.1016/j.cej.2021.132290>.

References

- [1] A. López-Díaz, A. Martín-Pacheco, A.M. Rodríguez, M.A. Herrero, A.S. Vázquez, E. Vázquez, Concentration gradient-based soft robotics: hydrogels out of water,

- Adv. Funct. Mater. 30 (46) (2020) 2004417, <https://doi.org/10.1002/adfm.v30.4610.1002/adfm.202004417>.
- [2] R. Luo, J. Wu, N.-D. Dinh, C.-H. Chen, Gradient porous elastic hydrogels with shape-memory property and anisotropic responses for programmable locomotion, Adv. Funct. Mater. 25 (47) (2015) 7272–7279, <https://doi.org/10.1002/adfm.v25.4710.1002/adfm.201503434>.
- [3] A.K. Mishra, T.J. Wallin, W. Pan, P. Xu, K. Wang, E.P. Giannelis, B. Mazzolai, R. F. Shepherd, Autonomic perspiration in 3D-printed hydrogel actuators, Sci. Robot. 5 (2020) eaaz3918, <https://doi.org/10.1126/scirobotics.aaz3918>.
- [4] M. Li, X. Wang, B. Dong, M. Sitti, In-air fast response and high speed jumping and rolling of a light-driven hydrogel actuator, Nat. Commun. 11 (2020) 3988, <https://doi.org/10.1038/s41467-020-17775-4>.
- [5] H. Zhang, Z. Li, C. Gao, X. Fan, Y. Pang, T. Li, Z. Wu, H. Xie, Q. He, Dual-responsive biohybrid neurobots for active target deliver, Sci. Robot. 6 (2021) eaaz9519, <https://doi.org/10.1126/scirobotics.aaz9519>.
- [6] O. Aydin, X. Zhang, S. Nuethong, G.J. Pagan-Diaz, R. Bashir, M. Gazzola, M.T. A. Saif, Neuromuscular actuation of biohybrid motile bots, PNAS 116 (40) (2019) 19841–19847, <https://doi.org/10.1073/pnas.1907051116>.
- [7] S. Liu, J. Wang, F.u. Tang, N.a. Wang, L. Li, C. Yao, L. Li, Aqueous systems with tunable fluorescence including white-light emission for anti-counterfeiting fluorescent inks and hydrogels, ACS Appl. Mater. Interfaces 12 (49) (2020) 55269–55277, <https://doi.org/10.1021/acsami.0c1681510.1021/acsami.0c16815.s001>.
- [8] S. Xie, C. Tong, H. Tan, N.a. Li, L. Gong, J. Xu, L. Xu, C. Zhang, Hydrothermal synthesis and inkjet printing of hexagonal-phase NaYF₄: Ln³⁺ upconversion hollow microtubes for smart anti-counterfeiting encryption, Mater. Chem. Front. 2 (11) (2018) 1997–2005, <https://doi.org/10.1039/C8QM00278A>.
- [9] S.-W. Tu, F.-C. Tsai, J.-K. Chen, H.-P. Wang, R.-H. Lee, J. Zhang, T. Chen, C.-C. Wang, C.-F. Huang, Preparations of tough and conductive PAMPS/PAA double network hydrogels containing cellulose nanofibers and polypyrroles, Polymers 12 (12) (2020) 2835, <https://doi.org/10.3390/polym12122835>.
- [10] C.-H. Wu, C.-W. Tu, J. Aimi, J. Zhang, T. Chen, C.-C. Wang, C.-F. Huang, Mechanochromic double network hydrogels as a compression stress sensor, Polym. Chem. 11 (2020) 6423–6428, <https://doi.org/10.1002/app.50949>.
- [11] W. Fan, C. Shan, H. Guo, J. Sang, R. Wang, R. Zheng, K. Sui, Z. Nie, Dual-gradient enabled ultrafast biomimetic snapping of hydrogel materials, Sci. Adv. 5 (4) (2019) eaav7174, <https://doi.org/10.1126/sciadv.aav7174>.
- [12] Y. Dong, J. Wang, X. Guo, S. Yang, M.O. Ozen, P. Chen, X. Liu, W. Du, F. Xiao, U. Demirci, B.F. Liu, Multi-stimuli-responsive programmable biomimetic actuator, Nat. Commun. 10 (2019) 4087, <https://doi.org/10.1038/s41467-019-10243-8>.
- [13] X. Peng, T. Liu, Q. Zhang, C. Shang, Q.-W. Bai, H. Wang, Surface patterning of hydrogels for programmable and complex shape deformations by ion inkjet printing, Adv. Funct. Mater. 27 (2017) 1701962, <https://doi.org/10.1002/anie.202013183>.
- [14] H. Qin, T. Zhang, N. Li, H.P. Cong, S.H. Yu, Anisotropic and self-healing hydrogels with multi-responsive actuating capability, Nat. Commun. 10 (2019) 2202, <https://doi.org/10.1038/s41467-019-10243-8>.
- [15] Y.u. Jiang, N. Hadjichristidis, Diels-Alder polymer networks with temperature-reversible cross-linking-induced emission, Angew. Chem. Int. Ed. 60 (1) (2021) 331–337, <https://doi.org/10.1002/anie.v60.110.1002/anie.202013183>.
- [16] J. Jin, H. Jiang, Q. Yang, L. Tang, Y. Tao, Y. Li, R. Chen, C. Zheng, Q. Fan, K. Y. Zhang, Q. Zhao, W. Huang, Thermally activated triplet exciton release for highly efficient tri-mode organic afterglow, Nat. Commun. 11 (2020) 842, <https://doi.org/10.1038/s41467-020-14669-3>.
- [17] K. Liu, X. Qiao, C. Huang, X. Li, Z. Xue, T. Wang, Spatial confinement tunes cleavage and re-formation of C=N bonds in fluorescent molecules, Angew. Chem. Int. Ed. 60 (26) (2021) 14365–14369, <https://doi.org/10.1002/anie.v60.2610.1002/anie.202103471>.
- [18] L. Song, T. Zhu, L. Yuan, J. Zhou, Y. Zhang, Z. Wang, C. Tang, Ultra-strong long-chain polyamide elastomers with programmable supramolecular interactions and oriented crystalline microstructures, Nat. Commun. 10 (2019) 1315, <https://doi.org/10.1038/s41467-019-09218-6>.
- [19] Z. Wu, J. Nitsch, J. Schuster, A. Friedrich, K. Edkins, M. Loebnitz, F. Dinkelbach, V. Stepanenko, F. Würthner, C.M. Marian, L. Ji, T.B. Marder, Persistent room temperature phosphorescence from triarylboranes: a combined experimental and theoretical study, Angew. Chem. Int. Ed. 59 (39) (2020) 17137–17144, <https://doi.org/10.1002/anie.v59.3910.1002/anie.202007610>.
- [20] C. Ma, W. Lu, X. Yang, J. He, X. Le, L. Wang, J. Zhang, M.J. Serpe, Y. Huang, T. Chen, Bioinspired anisotropic hydrogel actuators with on-off switchable and color-tunable fluorescence behaviors, Adv. Funct. Mater. 28 (7) (2018) 1704568, <https://doi.org/10.1002/adfm.v28.710.1002/adfm.201704568>.
- [21] S. Wei, W. Lu, X. Le, C. Ma, H. Lin, B. Wu, J. Zhang, P. Theato, T. Chen, Bioinspired synergistic fluorescence-color-switchable polymeric hydrogel actuators, Angew. Chem. Int. Ed. 58 (45) (2019) 16243–16251, <https://doi.org/10.1002/anie.v58.4510.1002/anie.201908437>.
- [22] Z. Li, P. Liu, X. Ji, J. Gong, Y. Hu, W. Wu, X. Wang, H.-Q. Peng, R.T.K. Kwok, J.W. Y. Lam, J. Lu, B.Z. Tang, Bioinspired simultaneous changes in fluorescence color, brightness, and shape of hydrogels enabled by AIEgens, Adv. Mater. 32 (11) (2020) 1906493, <https://doi.org/10.1002/adma.v32.1110.1002/adma.201906493>.
- [23] Y. Yao, C. Yin, S. Hong, H. Chen, Q. Shi, J. Wang, X. Lu, N. Zhou, Lanthanide-ion-coordinated supramolecular hydrogel inks for 3D printed full-color luminescence and opacity-tuning soft actuators, Chem. Mater. 32 (20) (2020) 8868–8876, <https://doi.org/10.1021/acs.chemmater.0c02448>.
- [24] H. Gao, Z. Zhao, Y. Cai, J. Zhou, W. Hua, L. Chen, L. Wang, J. Zhang, D. Han, M. Liu, L. Jiang, Adaptive and freeze-tolerant heteronetwork organohydrogels with enhanced mechanical stability over a wide temperature range, Nat. Commun. 8 (2017) 15911, <https://doi.org/10.1038/ncomms15911>.
- [25] X.-X. Le, Y.-C. Zhang, W. Lu, L.i. Wang, J. Zheng, I. Ali, J.-W. Zhang, Y.-j. Huang, M.J. Serpe, X.-T. Yang, X.-D. Fan, T. Chen, A novel anisotropic hydrogel with integrated self-deformation and controllable shape memory effect, Macromol. Rapid Commun. 39 (9) (2018) 1800019, <https://doi.org/10.1002/marc.v39.910.1002/marc.201800019>.
- [26] Z. Yang, W. Qin, N.L.C. Leung, M. Arseneault, J.W.Y. Lam, G. Liang, H.H.Y. Sung, I. D. Williams, B.Z. Tang, A mechanistic study of AIE processes of TPE luminogens: intramolecular rotation vs. configurational isomerization, J. Mater. Chem. C 4 (1) (2016) 99–107, <https://doi.org/10.1039/C5TC02924D>.
- [27] W. Zhao, Z. Liu, J. Yu, X. Lu, J.W.Y. Lam, J. Sun, Z. He, H. Ma, B.Z. Tang, Turning on solid-state luminescence by phototriggered subtle molecular conformation variations, Adv. Mater. 33 (2) (2021) 2006844, <https://doi.org/10.1002/adma.v33.210.1002/adma.202006844>.
- [28] Z. Zhao, J.W.Y. Lam, B.Z. Tang, Tetraphenylethene: a versatile AIE building block for the construction of efficient luminescent materials for organic light-emitting diodes, J. Mater. Chem. 22 (45) (2012) 23726, <https://doi.org/10.1039/c2jm31949g>.
- [29] M. Atanasov, B. Delley, D. Reinen, A DFT study of the energetical and structural landscape of the tetrahedral to square-planar conversion of tetrahalide complexes of copper(II), Z. Anorg. Allg. Chem. 636 (9–10) (2010) 1740–1750, <https://doi.org/10.1002/zaac.201000089>.
- [30] V. Peterson, G. Kearley, Y. Wu, A. Ramirez-Cuesta, E. Kemner, C. Kepert, Local vibrational mechanism for negative thermal expansion: a combined neutron scattering and first-principles study, Angew. Chem. Int. Ed. 49 (3) (2010) 585–588, <https://doi.org/10.1002/anie.200903366>.
- [31] T.-C. Wu, F.-Z. Zhao, Q.-L. Hu, Y.-S. Cui, T.-H. Huang, D. Zheng, Q. Liu, Y. Lei, L. Jia, C. Luo, Structural characterization, DFT studied, luminescent properties of cationic/neutral three-coordinated copper (I) complexes and application in warm-white light-emitting diode, Appl. Organomet. Chem. 34 (8) (2020), <https://doi.org/10.1002/aoc.v34.810.1002/aoc.5691>.